Microwave Imaging of Dielectric Cylinders Using the Multigrid Optimization Method

Mitsuru Tanaka, Toshiyuki Takada, and Kazuki Yano
Department of Electrical and Electronic Engineering, Oita University
700 Dannoharu, Oita-shi, Oita, 870-1192 Japan
E-mail: mtanaka@cc.oita-u.ac.jp

Abstract

This paper investigates the image reconstruction of lossy dielectric cylinders based on the multigrid optimization method (MGOM), which consists of the conjugate gradient method (CGM), the frequency-hopping technique (FHT), and the multigrid method (MGM). The inverse scattering problem is reduced to an optimization problem where a cost functional is minimized to obtain the contrast function. A fast reconstruction algorithm of estimating the relative permittivities of the objects is presented with multifrequency scattering data in microwave region. Some numerical results for dielectric circular cylinders confirm the effectiveness of the proposed method.

1. Introduction

Microwave imaging of unknown objects has attracted much attention in the study of nondestructive testing of materials, biomedical diagnosis, detection of underground objects, and radar target identification. In the past, several inversion methods have been developed to render the inverse problem tractable [1]-[14].

The purpose of this paper is to investigate an inverse scattering problem of imaging lossy dielectric cylinders based on the multigrid optimization method (MGOM). The MGOM is composed of the conjugate gradient method (CGM) [1], the frequency-hopping technique (FHT) [2], and the multigrid method (MGM) [15],[16]. We present a fast reconstruction algorithm of estimating the relative permittivities of the objects. We employ multifrequency scattering data in microwave region. As is well known [1], the inverse scattering problem consists of solving a nonlinear integral equation for a contrast function, which is expressed as a function of the relative permittivity of an object. We define a cost functional by the norm of the difference between the scattered electric fields measured and calculated. Then the inverse scattering problem is cast into an optimization problem where the contrast function is determined by minimizing the cost functional. Applying the MGOM to the optimization problem, one can derive an iterative algorithm for getting the contrast function. Computer simulations are performed for lossy dielectric circular cylinders to examine the validity of the proposed algorithm. It is seen from the numerical results that our procedure provides high-quality reconstructions with the property of fast convergence even for the case where the scattered data contains a measurement error.

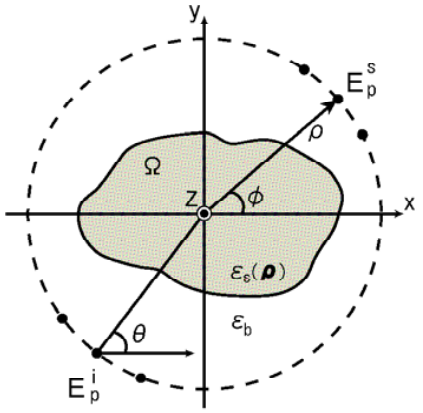

Fig. 1 Geometrical configuration of the problem.

2. Theory

A. *Inverse Scattering Problem*

Figure 1 shows the geometrical configuration of the problem. A lossy dielectric cylinder with relative permittivity $\varepsilon_s(\boldsymbol{\rho})$ and the cross section Ω is located in a homogeneous medium of relative permittivity ε_b. The object is illuminated by TM cylindrical electromagnetic waves $E_p^i(\theta;\, \boldsymbol{\rho})$ corresponding to the frequency of f_p, where $p = 1,\, 2, \cdots, P$. The incident waves are generated from line sources placed at points with polar coordinates $(\rho,\, \theta+\pi)$. The scattered electric fields $E_p^s(c;\, \theta;\, \boldsymbol{\rho})$ for each illumination are measured at the observation points with polar coordinates $(\rho,\, \phi)$. A contrast function, which characterizes the material property of the object, is written as

$$c(\boldsymbol{\rho}) = \varepsilon_s(\boldsymbol{\rho}) - \varepsilon_b. \tag{1}$$

The total electric field $E_p^t(c;\, \theta;\, \boldsymbol{\rho})$ inside the object, which is expressed as the sum of the incident electric field and the resulting scattered electric field, is represented as a solution to the linear integral equation,

$$E_p^t(c;\, \theta;\, \boldsymbol{\rho}) = E_p^i(\theta;\, \boldsymbol{\rho}) + k_p^2 \iint_{\Omega} c(\boldsymbol{\rho}') E_p^t(c;\, \theta;\, \boldsymbol{\rho}') \cdot G_p(\boldsymbol{\rho};\, \boldsymbol{\rho}')\, d\boldsymbol{\rho}', \quad \boldsymbol{\rho} \in \Omega. \tag{2}$$

The scattered electric field outside the object may be described by

$$E_p^s(c;\,\theta;\,\boldsymbol{\rho}) = k_p^2 \iint_{\Omega} c(\boldsymbol{\rho}')\, E_p^t(c;\,\theta;\,\boldsymbol{\rho}') \cdot G_p(\boldsymbol{\rho};\,\boldsymbol{\rho}')\, d\boldsymbol{\rho}', \quad \boldsymbol{\rho} \in \overline{\Omega}, \tag{3}$$

where $\overline{\Omega}$ indicates a domain outside the object, k_p is the free-space wavenumber for the frequency of f_p, and $G_p(\boldsymbol{\rho};\,\boldsymbol{\rho}')$ denotes the two-dimensional Green's function for the background medium given by

$$G_p(\boldsymbol{\rho};\,\boldsymbol{\rho}') = -\frac{j}{4} H_0^{(2)}(\sqrt{\varepsilon_b}\, k_p\, |\boldsymbol{\rho} - \boldsymbol{\rho}'|). \tag{4}$$

In Eq. (4), $H_0^{(2)}(\cdot)$ is the zeroth-order Hankel function of the second kind. The inverse scattering problem can be treated as the solution to the nonlinear integral equation for the contrast function, which is expressed as Eq. (3) by replacing $E_p^s(c;\,\theta;\,\boldsymbol{\rho})$ with the scattered electric field measured, $\widetilde{E}_p^s(\theta;\,\boldsymbol{\rho})$.

We suppose that the object is successively illuminated by incident waves for the frequency of f_p. The incident waves are generated from the line sources located at the points with angles $\theta = \theta_l$, where $l = 1, 2, \cdots, L$. For each illumination, the scattered electric fields are measured at observation points with angles $\phi = \phi_m$, where $m = 1, 2, \cdots, M$. The square investigation domain containing the object and the background medium is subdivided into $N \times N$ small square cells. The method of moments [17] is utilized to discretize Eqs. (2) and (3).

Let us define the following cost functional at the frequency of f_p:

$$F_p(c) = \sum_{l=1}^{L} \sum_{m=1}^{M} \left| E_p^s(c;\,\theta_l;\,\phi_m) - \widetilde{E}_p^s(\theta_l;\,\phi_m) \right|^2, \tag{5}$$

where $\widetilde{E}_p^s(\theta_l;\,\phi_m)$ and $E_p^s(c;\,\theta_l;\,\phi_m)$ are, respectively, the scattered electric fields measured and calculated at discrete points along a circle of radius ρ. Then the inverse scattering problem discussed here is reduced to an optimization problem where the contrast function is determined by minimizing the cost functional for P frequencies. Note that the measured data are simulated by solving the direct scattering problem for the true contrast function based on the FFT-CG method [18].

B. Multigrid Optimization Method

The optimization problem is solved by using the MGOM. Application of the CGM to the minimization of $F_p(c)$ at the frequency of f_p provides an iterative formula for estimating the contrast function. The gradient of $F_p(c)$ may be obtained from its Fréchet derivative [1]. The direction and the step size used in the CGM are determined by the Polak-Ribière-Polyak method and a univariate search technique [19],[20].

As is well known [2], the reconstruction accuracy degrades due to the property of nonlinearity inherent in the inverse scattering problem. The FHT employs the reconstructed result at the lower frequency as its initial estimate at the next higher frequency. Thus the effect of nonlinearity on the reconstructed image may be mitigated by using the FHT.

An inverse scattering problem usually takes much computational cost to obtain a convergent solution to a large set of nonlinear equations. The MGM is a fast solver for such a problem since it has the property that the oscillatory solution error can be rapidly decreased when the wavelength of the oscillation is comparable to the grid size [15],[16]. Then the relaxation calculation based on the CGM is performed for the suitable grid level in the MGM. Now we employ the MGM with V-cycle, which is constructed from two grid levels.

In the following, the parameters with the superscripts H and h denote the quantities obtained at the coarse grid level R^H and the fine grid level R^h, respectively. The reconstruction algorithm based on the MGOM is summarized as follows:

Step 0 Set an initial guess of c_p^H and $p = 1$.
Step 1 Apply ν_1 iterations to the minimization of $F_p(c)$ using the CGM at R^H: $min[\, F_p^H(c_p^H)\,] \rightarrow \hat{c}_p^H$.
Step 2 Interpolate $\hat{c}_p^H$ to c_p^h: $I_H^h \hat{c}_p^H \rightarrow c_p^h$.
Step 3 Apply ν_2 iterations to the minimization of $F_p(c)$ using the CGM at R^h: $min[\, F_p^h(c_p^h)\,] \rightarrow \hat{c}_p^h$.
Step 4 Restrict $\hat{c}_p^h$ to c_p^H: $I_h^H \hat{c}_p^h \rightarrow c_p^H$.
Step 5 Apply ν_3 iterations to the minimization of $F_p(c)$ using the CGM at R^H: $min[\, F_p^H(c_p^H)\,] \rightarrow \hat{c}_p^H$.
Step 6 Correct $\hat{c}_p^h$ using the difference between $\hat{c}_p^H$ and c_p^H: $\hat{c}_p^h + I_H^h(\,\hat{c}_p^H - c_p^H\,) \rightarrow c_p^h$.
Step 7 Apply ν_4 iterations to the minimization of $F_p(c)$ using the CGM at R^h: $min[\, F_p^h(c_p^h)\,] \rightarrow \hat{c}_p^h$.
Step 8 If two V-cycles are completed, then go to *Step 9*; else go to *Step 4*.
Step 9 Rstrict $\hat{c}_p^h$ to c_p^H and go to *Step 1* with $p := p+1$.

At the highest frequency of f_P, many V-cycles greater than two are exceptionally used until the relative residual error δ in the scattered electric field is finally less than a prescribed convergence criterion. In the above algorithm, I_h^H is the restriction operator converting a fine resolution to a coarse resolution. This operator gives a coarse-grid parameter using the four-point average of fine-grid parameters [15],[16]. On the other hand, I_H^h indicates the interpolation operator converting a coarse resoluton to a fine resolution. It produces a fine-grid parameter from coarse-grid parameters according to the well-known interpolation formula [15],[16]. For convenience, the proposed MGOM and the conventional CGM [1],[7] are called the method I and the method II, respectively. Note that the ralaxation calculations in the conventional CGM are performed only

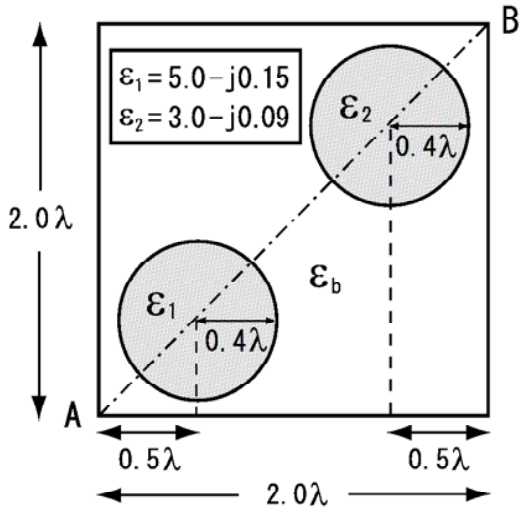

Fig. 2 Geometry for the simulations.

for the fixed fine grid level R^h.

3. Numerical Results

Computer simulations are made to examine the validity of the proposed method. We employ six frequencies of 1GHz, 2GHz, 3GHz, 4GHz, 5GHz, and 6GHz. Figure 2 presents the geometry for the simulations. Two dielectric circular cylinders with the same radius of 0.4λ have relative permittivities of $5.0 - j0.15$ and $3.0 - j0.09$, where λ is the free-space wavelength for the highest frequency of 6GHz. The current frequency hops to the next higher-frequency after two V-cycles are completed in the MGOM. The number of illuminations is 36 for one frequency, and the number of measurements of the scattered electric field is 36 for each illumination. The line sources and the observation points are equally spaced along a circle of radius 2λ. The $2\lambda \times 2\lambda$ investigation domain containing the object and the background free space is uniformly subdivided into 48×48 and 24×24 elementary square cells corresponding to R^h and R^H. The initial guess of the contrast function is zero, and the numbers of ν_1, ν_2, ν_3, and ν_4 are set to 5. Furthermore, a random noise with uniform distribution is added to the real and the imaginary parts of the scattered electric field to consider the effects of noise on the fidelity of reconstructed images. Now the signal-to-noise ratio (SNR) is 25dB.

Figure 3 shows the relative residual error δ in the scattered electric field versus the number of iterations. The solid and the dashed lines show the results based on the method I and the method II, respectively. Note that the number of iterations at the coarse grid level R^H is not counted due to the short computation time. Figures 4 and 5 illustrate the reconstructed results of the real part and the imaginary part of the relative permittivities of two dielectric circular cylinders along the diagonal $\overline{AB}$ with

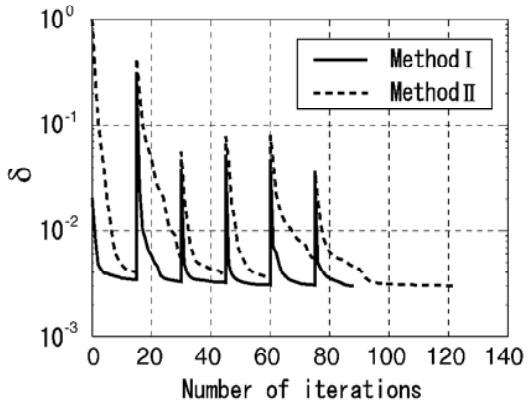

Fig. 3 Relative residual errors in the scattered electric field with SNR=25dB.

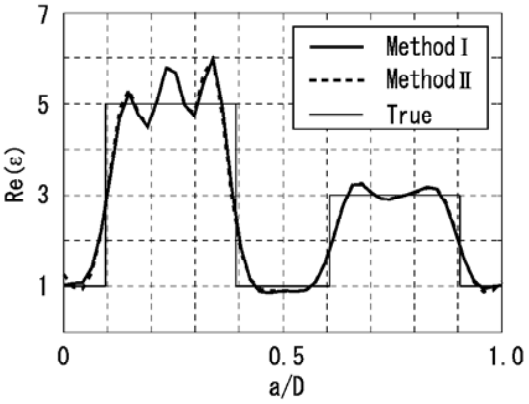

Fig. 4 Reconstructed results of the real part of complex relative permittivities of two dielectric circular cylinders with SNR=25dB.

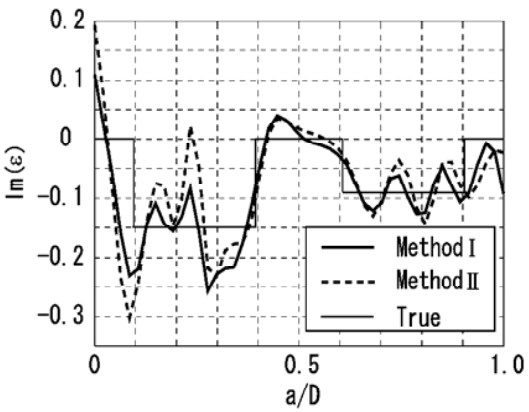

Fig. 5 Reconstructed results of the imaginary part of complex relative permittivities of two dielectric circular cylinders with SNR=25dB.

length of D. The parameter a in these figures indicates the distance from the initial point A along this diagonal. The reconstructions presented in Figs. 4 and 5 are the results after 88 and 122 iterations corresponding to the method I and the method II. The final convergence criterion for δ is $\delta \leq 3 \times 10^{-3}$. For reference, the true profiles of the real and the imaginary parts of the relative permittivities are also shown by the thin solid lines in Figs. 4 and 5.

It is seen from Figs. 3-5 that the rate of convergence for the proposed method is much faster than that for the conventional CGM to achieve the same reconstruction accuracy.

4. Conclusion

Microwave imaging of lossy dielectric cylinders based on the MGOM has been investigated. We present an iterative reconstruction algorithm of estimating the relative permittivities of the objects. Simulated results are presented for dielectric circular cylinders using the multifrequency scattering data. The results confirm that the proposed method provides high-quality reconstructions with the property of much faster convergence than the conventional CGM. Study on the utilization of multigrid methods with many grid levels and different cycles remains a topic for further study.

References

[1] H. Harada, D. J. N. Wall, T. Takenaka, and M. Tanaka, "Conjugate gradient method applied to inverse scattering problem," IEEE Trans. Antennas & Propag., vol. 43, no. 8, pp. 784–792, Aug. 1995.

[2] W. C. Chew and J. H. Lin, "A frequency-hopping approach for microwave imaging of large inhomogeneous bodies," IEEE Microwave & Guided Wave Lett., vol. 5, no. 12, pp. 439–441, Dec. 1995.

[3] C.-S. Park, S.-K. Park, and J.-W. Ra, "Moment method and iterative reconstruction of two-dimensional complex permittivity by using effective modes with multiple sources in the presence of noise," Radio Sci., vol. 31, no. 6, pp. 1877–1886, Nov.-Dec. 1996.

[4] A. Franchois and C. Pichot, "Microwave imaging—Complex permittivity reconstruction with a Levenberg-Marquardt method," IEEE Trans. Antennas & Propag., vol. 45, no. 2, pp. 203–215, Feb. 1997.

[5] K. Belkebir, R. E. Kleinman, and C. Pichot, "Microwave imaging—Location and shape reconstruction from multifrequency scattering data," IEEE Trans. Microwave Theory & Tech., vol. 45, no. 4, pp. 469–476, April 1997.

[6] Z.-Q. Meng, T. Takenaka, and T. Tanaka, "Image reconstruction of two-dimensional impenetrable objects using genetic algorithm," J. Electromag. Waves & Appl., vol. 13, no. 1, pp. 95–118, Jan. 1999.

[7] H. Harada, M. Tanaka, and T. Takenaka, "Image reconstruction of a three-dimensional dielectric object using a gradient-based optimization," Microwave & Opt. Technol. Lett., vol. 29, no. 5, pp. 332–336, June 2001.

[8] M. Tanaka and K. Ogata, "Fast inversion method for electromagnetic imaging of cylindrical dielectric objects with optimal regularization parameter," IEICE Trans. Commun., vol. E84-B, no. 9, pp. 2560–2565, Sept. 2001.

[9] A. Abubakar, P. M. van den Berg, and J. J. Mallorqui, "Imaging of biomedical data using a multiplicative regularized contrast source inversion method," IEEE Trans. Microwave Theory & Tech. vol. 50, no. 7, pp. 1761–1770, July 2002.

[10] A. Qing, "Electromagnetic imaging of two-dimensional perfectly conducting cylinders with transverse electric scattered field," IEEE Trans. Antennas & Propag., vol. 50, no. 12, pp. 1786-1794, Dec. 2002.

[11] S. Caorsi, M. Donelli, and A. Massa, "Detection, location, and imaging of multiple scatterers by means of the iterative multiscaling method," IEEE Trans. Microwave Theory & Tech., vol. 52, no. 4, pp. 1217–1228, April 2004.

[12] S. Y. Semenov, A. E. Bulyshev, A. Abubakar, V. G. Posukh, Y. E. Sizov, A. E. Souvorov, P. M. van den Berg, and T. C. Williams, "Microwave-tomographic imaging of the high dielectric-contrast objects using different image-reconstruction approaches," IEEE Trans. Microwave Theory & Tech., vol. 53, no. 7, pp. 2284–2294, July 2005.

[13] J.-L. Hu, Z. Wu, H. McCann, L. E. Davis, and C.-G. Xie, "Sequential quadratic programming method for solution of electromagnetic inverse problems," IEEE Trans. Antennas & Propag., vol. 53, no. 8, pp. 2680–2687, Aug. 2005.

[14] D. Franceschini, M. Donelli, G. Franceschini, and A. Massa, "Iterative image reconstruction of two-dimensional scatterers illuminated by TE waves," IEEE Trans. Microwave Theory & Tech., vol. 54, no. 4, pp. 1484–11494, April 2006.

[15] W. L. Briggs, V. E. Henson, and S. F. McCormick, *A multigrid tutorial, Second Edition*, SIAM, 2000.

[16] U. Trottenberg, C. W. Oosterlee, and A. Schüller, *Multigrid*, Academic Press, 2001.

[17] R. F. Harrington, *Field computation by moment methods*, Macmillan, New York, 1968.

[18] D. T. Borup and O. P. Gandhi, "Calculation of high-resolution SAR distributions in biological bodies using the FFT algorithm and conjugate gradient method," IEEE Trans. Microwave Theory & Tech. vol. 33, no. 5, pp. 417–419, May 1985.

[19] S. L. S. Jacoby, J. S. Kowalik, and J. T. Pizzo, *Iterative methods for nonlinear optimization problems*, Prentice-Hall, Englewood Cliffs, 1972.

[20] H. Konno and H. Yamashita, *Nonlinear planning method*, Nikkagiren, 1990 (*in Japanese*).